ACS NANO

www.acsnano.org

Phyto-Courier, a Silicon Particle-Based Nano-biostimulant: Evidence from *Cannabis sativa* Exposed to Salinity

Gea Guerriero, Flavia Maria Sutera, Nissim Torabi-Pour, Jenny Renaut, Jean-Francois Hausman, Roberto Berni, Holly Cherise Pennington, Michael Welsh, Ashkan Dehsorkhi, Lali Ronsoni Zancan, and Suzanne Saffie-Siebert*

Cite This: *ACS Nano* 2021, 15, 3061–3069

Read Online

ACCESS | Metrics & More | Article Recommendations | Supporting Information

ABSTRACT: **Global warming and sea level rise are serious threats to agriculture. The negative effects caused by severe salinity include discoloration and reduced surface of the leaves, as well as wilting due to an impaired uptake of water from the soil by roots. Nanotechnology is emerging as a valuable ally in agriculture: several studies have indeed already proven the role of silicon nanoparticles in ameliorating the conditions of plants subjected to (a) biotic stressors. Here, we introduce the concept of phyto-courier: hydrolyzable nanoparticles of porous silicon, stabilized with the nonreducing saccharide trehalose and containing different combinations of lipids and/or amino acids, were used as vehicle for the delivery of the bioactive compound quercetin to the leaves of salt-stressed hemp (*Cannabis sativa* L., Santhica 27). Hemp was used as a representative model of an economically important crop with multiple uses. Quercetin is an antioxidant known to scavenge reactive oxygen species in cells. Four different silicon-based formulations were administered *via* spraying in order to investigate their ability to improve the plant's stress response, thereby acting as nano-biostimulants. We show that two formulations proved to be effective at decreasing stress symptoms by modulating the amount of soluble sugars and the expression of genes that are markers of stress-response in hemp. The study proves the suitability of the phyto-courier technology for agricultural applications aimed at crop protection.**

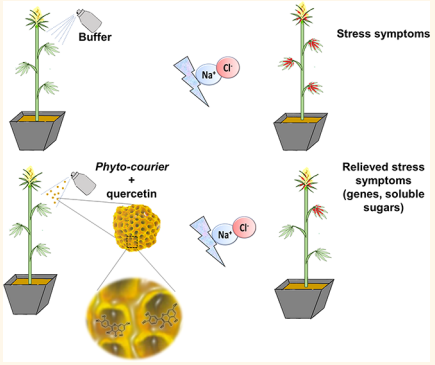

KEYWORDS: *hybrid silicon nanoparticles, nanobiostimulants, salinity, Cannabis sativa, agriculture, crop protection*

Abiotic stress constitutes a severe threat to crops as it impacts growth and, consequently, productivity.[1] Among the top-ranking stresses of abiotic nature, salinity deserves special attention, considering that sea levels rise at an alarming average of >3 mm per year.[2] Therefore, ensuring agricultural productivity under changing environmental conditions is a societal challenge of the utmost importance and urgency.[3] Salinity causes secondary stresses in plants, notably osmotic imbalances, nutrient deficiency, and oxidative stress.[4] The absorption of water decreases as a result of the lowered soil osmotic potential due to salt, and this, in turn, causes a decreased uptake of nutrients with consequences on growth and development. High salinity also causes oxidative stresses to plant tissues because of the induction of reactive oxygen species (ROS), which are scavenged by means of enzymatic [*e.g.*, superoxide dismutase (SOD), glutathione reductase (GR), ascorbate peroxidase (APX)] and non-enzymatic systems (for example, through the synthesis of flavonoids).[5]

The impact of salinity is of economic importance in the case of multipurpose crops, that is, plants that are used in different industrial sectors. One such model is industrial hemp, *Cannabis sativa* L., grown both for fibers and for seed oil. Hemp is also a treasure trove of specialized metabolites with known pharmacological interest, namely, cannabinoids and phenolic compounds,[6] such as cannflavins and lignanamides.[7,8]

It was previously shown by us that hemp growth and development was affected by salinity, which decreased the number of both primary and secondary bast fibers in the stems,[9] affected the leaf biomass, and impacted the xylem vessels' lumen by making them smaller.[10] At the gene level,

Received: November 12, 2020
Accepted: January 20, 2021
Published: February 1, 2021

https://dx.doi.org/10.1021/acsnano.0c09488
ACS Nano 2021, 15, 3061–3069

salt-stressed hemp leaves were characterized by an up-regulation of transcripts involved in secondary cell wall formation (cellulose synthase gene *CesA4*), together with the lignification-related genes [*i.e.*, cinnamyl alcohol dehydrogenase (*CAD*) and phenylalanine ammonia lyase (*PAL*)]. An increase in stress-responsive genes partaking in ethylene response (ethylene response factor 1, *ERF1*) and protein folding (heat shock proteins *HSP70* and *HSP81.4*) was also observed.[10]

The root application of silicon (Si) in the form of 2 mM sodium metasilicate was recently shown to mitigate stress symptoms in the leaves of salt-exposed *C. sativa* plants, where older fan leaves showed xylem vessels with a wider lumen compared to plants that did not receive Si.[11]

Si is a quasi-essential metalloid whose role in protecting against stress is well-documented and is in large part due to its association, as silica, with plant cell walls.[12,13] Hemp is not a Si accumulator but can deposit Si in its stems and leaves[14] and has aquaporins orthologous to the *Lsi1* gene from rice.[15] *C. sativa* subjected to abiotic stresses (salinity and heavy metals) showed an improvement of the stress symptoms.[16] It is therefore a suitable model of a multipurpose crop to study the response to both salinity and Si application.

The use of nanotechnology already showed promising results for the management of biotic stress, for example, by decreasing the spread of chemicals or by improving the soil quality and stimulating the growth of plants.[17] Additionally, the efficacy of lignin-based nanocarriers loaded with fungicides was demonstrated in the treatment of the grapevine trunk disease Esca.[18] The lignin nanocarriers can be injected at the site of infection where fungi degrade them by secreting ligninolytic enzymes, thereby promoting the release of the fungicide. It was shown that only small amounts of fungicide (<10 mg) are needed to cure an infected tree, and that only Esca-infected trees trigger the release of the fungicide.

In addition to lignin nanocarriers, Si nanoparticles (Si-NPs) are also used in crop protection for the delivery of different molecules, namely, nucleic acids, proteins, or chemicals.[19] Si-based formulations belong to the category of biostimulants in EU regulations[20,21] and have been applied as foliar sprays for crop protection for three decades.

In the present study, hydrolyzable porous Si-NPs combined with trehalose (and referred to as phyto-courier) were prepared and used as carrier systems of the flavonoid quercetin to study whether they mitigated the stress symptoms in the leaves of textile hemp subjected to salt stress. Trehalose, a nonreducing disaccharide acting as osmo-protectant, has demonstrated efficacy in alleviating stress-induced symptoms in several plants.[22−25] Additionally, its role in improving plant tolerance in the presence of salt-induced oxidative stress has been investigated in several commercial crops, including wheat and rice.[26,27] This disaccharide is also an ideal lyoprotectant used in the formulation of nanosized liposomes.[28]

Quercetin was chosen in the light of the available literature data on its use as a stress-mitigating compound in plants. This flavonoid was indeed shown to protect thale cress, tobacco, and *Lemna gibba* against oxidative stresses caused by Paraquat by reducing carbonylated proteins and stabilizing the chlorophyll content.[29] Additionally, the provision of quercetin also protected tomato against the oxidative damages of salinity by inducing the antioxidant enzymatic system and by increasing the root/shoot fresh and dry weight.[4] Quercetin thus shows properties that are equivalent to those of natural extracts falling under the category of plant biostimulants.

The results presented here prove that the Si-based phyto-courier containing quercetin conferred protection to hemp leaves against salt stress by affecting the content of some soluble sugars and the expression of stress-responsive genes. Among the four different formulations (indicated by GS1−GS2−GS3−GS4), GS1 and GS2 showed the best stress-mitigating effects both macroscopically and from a molecular point of view.

The results demonstrate the suitability of the Si-based phyto-courier in acting as a nanobiostimulant and in mitigating the stress response in hemp. Follow-up studies will address whether other administration routes (*i.e.*, root amendment) are more effective and whether other types of compounds and mixtures thereof can be used for the functionalization of the phyto-courier.

RESULTS AND DISCUSSION

Si-NPs and Phyto-Couriers' Characterization. Si-NPs (purity above 98%), after being subjected to methanolic rinsing and a slow evaporation process, were characterized for the available surface of the particles, particle size, and residual solvent. The average available surface was determined to be approximately 34.8 m^2/g, and the average particle size measured by transmission electron microscopy (TEM) had a size of <100 nm (Figure 1). The methanol (MeOH) content

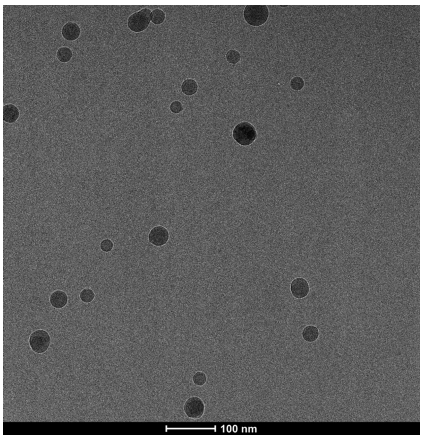

Figure 1. Transmission electron microscopy picture of the nanoporous Si after MeOH rinsing and a slow evaporation process.

was assessed to be less than 3000 ppm and in line with ICH (International Council for Harmonization of Technical Requirements for Pharmaceuticals for Human Use) specifications.

The zeta-potential of Si-NPs was determined to be −30.4 ± 3.3 mV and accounted for the expected negative charge of porous Si material that relates to the presence of hydroxyl groups on the surfaces of the Si-NPs.

After formulating the Si-based phyto-courier according to the process described above, the samples were analyzed again for residual solvents: the MeOH level was determined to be less than 3000 ppm, whereas ethanol (EtOH) was less than 5000 ppm.

The quercetin content in the samples was determined prior to *in planta* studies and was found to be in the range of 95−105% with respect to the nominal content.

https://dx.doi.org/10.1021/acsnano.0c09488
ACS Nano 2021, 15, 3061−3069

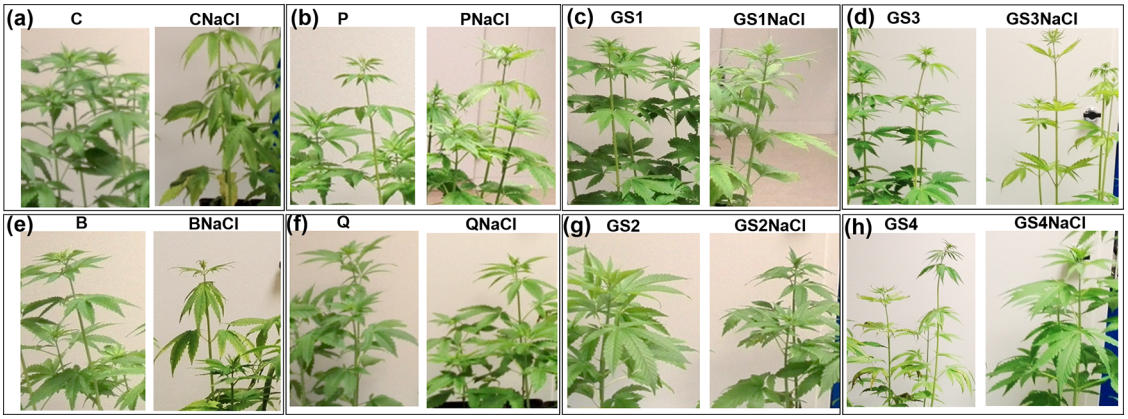

Figure 2. Macroscopic phenotypes of plants aged 27 days grown in the absence/presence of 250 mM NaCl and treated with the phyto-courier formulations. C, control; B, buffer; P, phyto-courier alone; Q, quercetin alone; GS1−GS4, phyto-courier formulations containing quercetin. NaCl: stressed plants.

Phenotype, Leaf Fresh/Dry Weights, and Moisture Percentage. Comparisons of the control (C) *versus* treated plants in the absence of NaCl showed no noticeable differences when all of the phyto-courier formulations were compared, while under salt exposure, an amelioration of the stress signs could be noticed in the plants treated with the hybrid formulations GS1 and GS2 (Figure 2). Indeed, drooping of the leaves was very evident in the salt-exposed plants that were not subjected to any treatment, as well as in those treated with B (Figure 2a,b). The phenotype was even more evident in plants aged 31 days (Figure S1a,b). The phenotype was less marked in the hemp plants that had been sprayed with the hybrid formulations GS1 and GS2 (Figure 2e,f and Figure S1e,f): in those, the leaves were indeed more turgid. The plants treated with the formulations GS3 and GS4, despite having more turgid leaves than those treated with buffer alone (Figure 2g,h), showed necrotic tips (Figure S2g,h). Plants treated with Q (quercetin alone) or with P (phyto-courier alone without the active ingredient quercetin) showed less evident signs of stress compared to those that received no treatment or that were sprayed with the buffer (Figure 2c,d).

For two formulations (*i.e.*, GS3 and GS4), some leaf discoloration was already noticeable on plants aged 20 days (Figure S2): the tips of the leaves showed intravein discoloration on the dorsal side. The phenotype was particularly evident under salt exposure. A possible explanation of this phenotype is provided by considering the different discrete amounts of quercetin taken up by the leaf epidermal cells following the application of the phyto-courier formulations GS3 and GS4 compared to GS1 and GS2. A faster and/or greater entrapment may have caused quercetin overfeeding, which led to high levels of oxidation of the flavonoid (with pro-oxidant effects), especially under salt exposure (Figure S1g,h).

The leaf fresh weight (FW) of plants that were subjected to salinity was lower than that of C plants; this difference was statistically significant, with the exception of plants that were sprayed with P, GS2, and GS4, for which the differences were not significant (Figure S3).

The dry weight (DW), however, showed no statistically significant changes, except for the pairwise comparisons of GS1 *versus* GS1 NaCl, where the differences were significant after the ANOVA one-way and Tukey's posthoc test (Figure S3b). As Si applied *via* roots and foliar spraying was shown to maintain the relative water content in plants under water deficit,[30] the leaf moisture percentage was measured (Figure S3c). The control leaves or those treated with B showed statistically significant decreases in moisture content under stress; however, for P, Q, GS1, GS2, GS3, and GS4, the differences between unstressed and stressed conditions were not significant (Figure S3c). It should be noted that this result was in agreement with the visual inspection described previously (Figure 2 and Figure S1). A higher standard deviation was, however, present in the DW of stressed samples treated with GS3 and GS4, and a tendency toward a decrease could be observed.

Si Quantification in *C. sativa* Leaves. Si contents did not show statistically significant changes among the leaves that were not sprayed or sprayed with buffer alone and those treated with the four phyto-courier formulations GS1−GS4, both in the absence and presence of salt stress (Figure S4). The only exception was represented by the nonstressed leaves sprayed with the phyto-courier alone (P). This difference is not meaningful in physiological terms, as the leaves are not the main organs responsible for Si absorption (the cuticle represents a barrier to the diffusion of substances) and may be due to the high variation among the four biological replicates in the control (C) and buffer (B) conditions. It should also be noted that, although hemp was previously shown to accumulate Si in the leaves,[11,14] it cannot be considered a silicifier. The content of Si after fertilization with sodium metasilicate increased from 0.34 to 0.66% DW.[11] Rice, a known silicifier, was reported to contain up to 10% of the shoot DW.[31]

The phyto-courier degrades over time, thereby releasing the active ingredient (in this case quercetin) and orthosilicic acid (OSA). OSA is the Si form taken up by plants *via* the roots, through aquaporins belonging to the family of Nodulin-26-like intrinsic proteins (NIPs).[15] Studies on Si foliar spraying are available for several crops and mainly in relation to biotic stress;[20] in tomato, rice, finger millet, and sugar cane, the highest Si content was recorded in sprays containing 4 mL/L PEG stabilized silicic acid (corresponding to 30 ppm of Si).[20] In our experimental setup, the amount of Si delivered *via* one spraying is estimated to be 6.4 ppm: the low amount of Si detected is thus explained by the low doses delivered *via* spraying.

Content of Soluble Sugars. The quantification of the soluble sugars showed a response in salt-stressed hemp leaves

https://dx.doi.org/10.1021/acsnano.0c09488
ACS Nano 2021, 15, 3061−3069

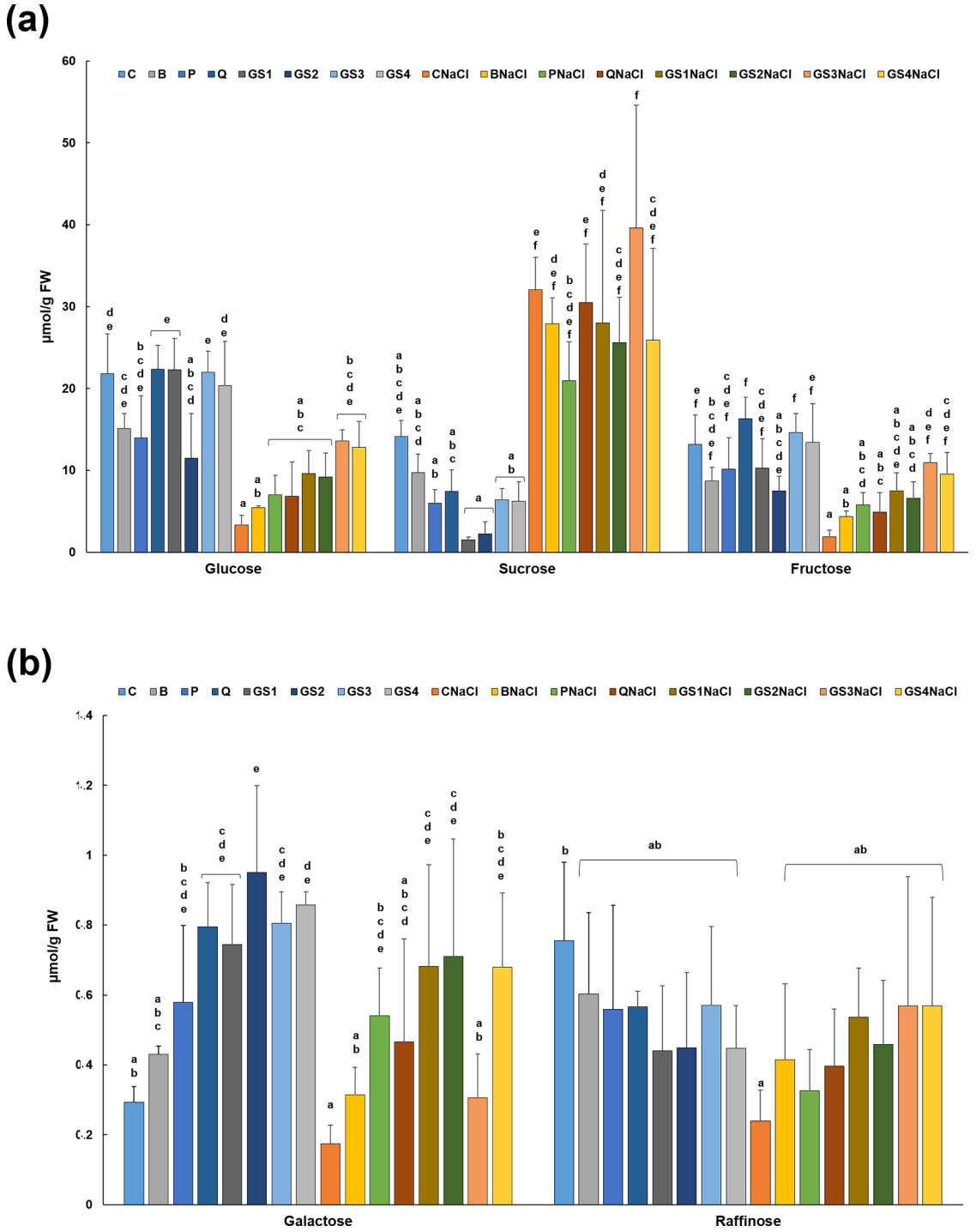

Figure 3. Content of soluble sugars (expressed as μmol/g of FW), namely, glucose, sucrose, and fructose (a) and galactose and raffinose (b) in the leaves of plants treated or not with the formulations under control or salt stress conditions. Error bars correspond to the standard deviation calculated from four biological replicates. Different letters on the vertical bars indicate statistically significant differences ($p < 0.05$) among groups. An ANOVA one-way followed by Tukey's posthoc test was used for raffinose results [$F(15,48) = 1.53$, p-value = 0.133], whereas a Kruskal–Wallis test with Dunn's posthoc test was applied to glucose [$X^2(15) = 52.03$, p-value = 0.000], fructose [$X^2(15) = 47.11$, p-value = 0.000], sucrose [$X^2(15) = 54.58$, p-value = 0.000], and galactose [$X^2(15) = 40.79$, p-value = 0.000]) data. C, control; B, buffer; P, phyto-courier alone; Q, quercetin alone; GS1–GS4, phyto-courier formulations containing quercetin. NaCl: stressed plants.

entailing a decrease of glucose and fructose and an increase in the content of sucrose (Figure 3). One of the mechanisms activated in response to salinity in plants is the increased content of sugars which act as osmo-protectants.[32]

In salt stress conditions, glucose showed a tendency toward increase in BNaCl *versus* GS3NaCl and BNaCl *versus* GS4NaCl, but the differences were not statistically significant because of the high standard deviation, while fructose increased significantly in BNaCl *versus* GS3NaCl and BNaCl *versus* GS4NaCl (Figure 3a).

Sucrose increased significantly in the leaves treated with Q, GS1, GS2, GS3, and GS4 under salt stress. However, when

https://dx.doi.org/10.1021/acsnano.0c09488
ACS Nano 2021, 15, 3061–3069

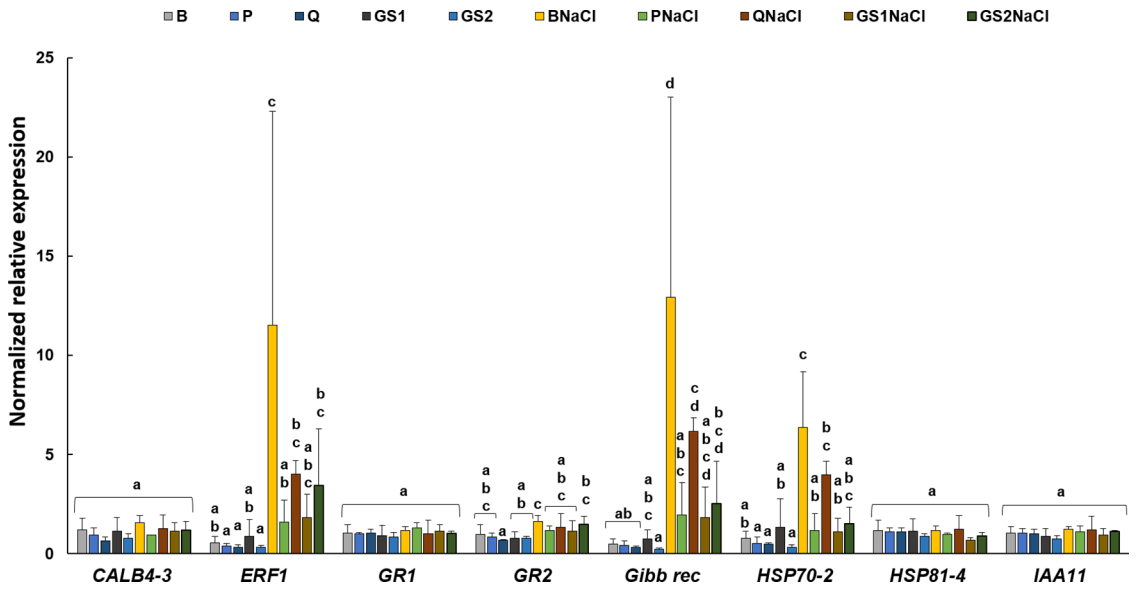

Figure 4. Gene expression analysis (expressed as normalized relative expression) in the leaves of plants treated or not with the formulations under control or salt stress conditions. Error bars correspond to the standard deviation calculated from four biological replicates. Different letters on the vertical bars indicate statistically significant differences ($p < 0.05$) among groups (the data were $\log_{10}$-transformed and tested for normal distribution and homogeneity). Then an ANOVA one-way analysis followed by Tukey's posthoc test was applied for *ERF1* [$F(9,29) = 8.17$, p-value = 0.000], *GR2* [$F(9,29) = 4.75$, p-value = 0.001], *Gibb rec* [$F(9,29) = 9.26$, p-value = 0.000], *HSP70-2* [$F(9,29) = 7.84$, p-value = 0.000], and *IAA* [$F(9,29) = 1.52$, p-value = 0.187], whereas a Kruskal–Wallis test with Dunn's posthoc test was applied for *CALB4-3* [$X^2(9) = 13.10$, p-value = 0.158], *GR1* [$X^2(9) = 7.57$, p-value = 0.578], and *HSP81-4* [$X^2(9) = 15.66$, p-value = 0.0740]). C, control; B, buffer; P, phyto-courier alone; Q, quercetin alone; GS1–GS4: phyto-courier formulations containing quercetin. NaCl: stressed plants.

comparing the sucrose levels in stressed *versus* nonstressed leaves treated with GS1 and GS2, the fold change was higher than that in GS3 and GS4: the increase was 18- and 11.5-fold under salt stress for GS1 and GS2, whereas it was 6- and 4-fold in GS3 and GS4, respectively. The sucrose levels increased 2.8-fold under salinity in the leaves treated with B alone.

The higher increase observed for GS1 and GS2 is due to lower values of sucrose in the nonstressed leaves treated with these products (Figure 3a). These phyto-courier formulations may induce the activity of sucrose-metabolizing enzymes which generate the UDP-glucose required, among others, for cellulose biosynthesis.

Galactose increased significantly in the leaves sprayed with GS2 and GS4, compared to those sprayed with B alone, whereas raffinose did not show any statistically significant changes (Figure 3b).

Gene Expression Analysis. To determine, from a molecular perspective, whether the formulations protected the leaves after salt exposure, a subset of genes involved in the response to exogenous constraints and previously studied on hemp was chosen.[10,11] The molecular analyses were carried out on the plants sprayed with B, Q, P, GS1, and GS2. These conditions were chosen because of the evident macroscopic effects of GS1 and GS2 compared to the leaves sprayed with B alone and the absence of discoloration (Figures S1c,g and S2e,f) and in the light of the higher induction of sucrose levels under salt stress (Figure 3a).

The genes targeted encode the calcium-dependent lipid-binding family protein isoform 4-3 (CALB4-3), the ethylene response factor ERF1, two glutathione reductases (GR), the gibberellin receptor (Gibb rec), the heat shock proteins HSP70-2 and HSP81-4, and the auxin-responsive protein (IAA11).

The statistical tests highlighted the occurrence of significant decreases in the expression of *ERF1* in BNaCl *versus* PNaCl, *Gibb rec* in BNaCl *versus* PNaCl, and *HSP70-2* in BNaCl *versus* PNaCl and BNaCl *versus* GS1NaCl (Figure 4). Although not significant, lower values in gene expression were also observed for the stressed leaves that had received the treatment with GS2.

The gene expression results indicated an amelioration of the formulations GS1 and GS2 and of P in the response to salt exposure: NaCl is known to cause oxidative stress, which results in the activation of genes involved in phytohormone signaling, that is, ethylene and gibberellin which are particularly important in young tissues,[33] as is the case for the tissues sampled here for qPCR analysis, and in macromolecules' protection (*i.e.*, HSPs). The decreased expression observed after the treatment with P, GS1, and GS2 suggests mitigation of oxidative stress in the treated leaves.

CONCLUSIONS

Ensuring crop productivity under adverse environmental conditions is an important challenge for agriculture. Nanotechnology can offer solutions to this problem, although safety and health aspects are a matter of debate. Here, the concept of phyto-courier is introduced: hydrolyzable Si-NPs in a hybrid system were used to deliver the flavonoid quercetin to textile hemp stressed by salinity. The results indicate a protective effect of the hybrid formulations GS1 and GS2 against NaCl. The leaves treated with these phyto-courier formulations accumulated higher levels of sucrose and showed a decreased expression of genes related to abiotic stress response. The results warrant follow-up studies to test additional administration routes (*e.g.*, soil drenching). Different exposure time windows and frequencies need to be evaluated, too, to avoid

https://dx.doi.org/10.1021/acsnano.0c09488
ACS Nano 2021, 15, 3061–3069

Table 1. Composition of Tested Si-Based Formulations and Related Controls[a]

sample name	Si (mg)	trehalose (mg)	quercetin (mg)	phosphatidyl choline (mg)	arginine (mg)	glycine (mg)	total formulation volume (mL)
GS1	4	4	2.5	16	4	2	50
GS2	4	4	2.5		4	2	50
GS3	4	4	2.5	16			50
GS4	4	4	2.5				50
GS5 (referred to as Q)			2.5				50
GS6 (referred to as P)	4	4					50
GS7 (referred to as B)							50

[a]Note: a fixed 1:1 weight ratio of Si-NPs to trehalose was used in all Si-based formulations. The vehicle is constituted by a viscous spray solution containing hypromellose and Pluronic L-61 at 0.01% (w/v) concentration in the finished product.

the occurrence of leaf discolorations, such as those observed for the hybrid formulations GS3 and GS4.

METHODS

Preparation of the Si-Based Phyto-Courier Hybrid Formulations by Slow Evaporation and Assessment of Surface Area, Particle Size, and Residual Solvent. The Si-based hybrid carrier system was prepared with various compositions. Si-NPs were sourced from a number of suppliers (Si nanopowder, purity ≥98%, Sigma-Aldrich, UK and Zhengzhou Dongyao Nano Materials, China).[34]

L-α-Phosphatidylcholine (from soybean), trehalose (purity >99.0%), quercetin (purity >99.0%), glycine (ACS reagent, purity >98.5%), and arginine (L-Base, purity >98.0%), phosphate-buffered saline (PBS tablets), hypromellose 2910, and Pluronic L-61 (average M_n ~ 2000) were purchased from Sigma-Aldrich, UK. Methanol (MeOH, HPLC grade) and ethanol (EtOH, HPLC grade) were purchased from Rathburn, UK. For analysis, EtOH and MeOH GC standards were purchased from Sigma-Aldrich, UK; trifluoroacetic acid was obtained from Tokyo Chemical Industries (TCI, Hong Kong).

Si-NPs were assessed and compared in preliminary studies and determined to be suitable for use, with the Zhengzhou Dongyao material used for the study *in planta*.

Si-NPs (500 g) were preliminary rinsed with 500 mL of MeOH, gently stirred for 2 h, and then subjected to a slow evaporation technique until dryness was reached.[34−39] Subsequently, Si-NPs were characterized for surface area, particle size, and residual solvent prior to further formulation of the phyto-courier.

Surface area analysis was performed by gas sorption using a Quantachrome Nova 2200e and calculated according to the Brunauer−Emmett−Teller theory. Before the measurements, the samples were degassed at 350 °C o/n.

TEM was used to visually examine the size and structure of the Si-NPs. The particle suspension was diluted to 0.01% (w/v) in deionized water, and a drop of sample was dried at reduced temperature under vacuum over a carbon-coated copper grid. The samples were then observed at an accelerating voltage of 100 kV under an FEI Talos L120C G2 TEM.

The surface charge of Si-NPs was determined by means of zeta-potential using a ZetaSizer Nano ZS (Malvern Panalytical, UK). All measurements were undertaken in deionized water. Samples were sufficiently diluted to yield a count rate at a range of 100−400 kcps. All measurements were made at 25 °C in triplicate and reported as means ± standard deviation.

Solvent residual analysis was performed *via* a Shimadzu GC-2030 connected to an FID detector, using a Shimadzu RTx-624 column. Autosampler/headspace conditions were as follows: incubation 80 °C for 60 min, syringe temperature 90 °C, 250 rpm, prepurge time 30 s, injection flow rate 10 mL/min. Injector conditions were as follows: hydrogen as gas carrier, 140 °C, split ratio 5:1, carrier gas linear speed 35 cm/s; oven temperature = baseline at 40 °C for 12 min, then ramp/rate 16.7 °C/min for 12 min then held at 240 °C for 12 min; FID temperature = 250 °C, nitrogen flow 30 mL/min, air flow 400 mL/min.

A standard curve of EtOH was made for quantification using the EtOH stock standard and deionized water at the concentrations of 25−75−150−500−1000−5000 ppm. A blank was prepared by simply injecting deionized water. One milliliter of each standard concentration was accurately measured into a headspace vial and capped. For MeOH, an ampule of residual solvent MeOH reference standard and deionized water was used to prepare a standard curve at the concentrations of 50−100−150−300−1000−3000 ppm. A blank was prepared by simply injecting deionized water. One milliliter of each standard concentration was thoroughly measured into a headspace vial and capped.

To determine the residual solvent in the prepared samples, 1 mg of the sample was weighed into a GC headspace vial. Thereafter, 1 mL of deionized water was added and the sample vial was capped with a magnetic lid and analyzed.

Inductively coupled plasma mass spectrometry (ICP-MS) analysis was performed to determine the concentration of ^{28}Si in the Si-NPs.[34,40]

Formulation of the Phyto-Couriers. Hybrid formulations were made, where appropriate, by creating a lipid film using a rotary evaporator. L-α-Phosphatidylcholine was solubilized in a sufficient quantity of EtOH and then subjected to solvent evaporation by rotary evaporation (Heidolph Laborota 4001). The film was rehydrated with premixed quercetin, trehalose, amino acids, and activated Si particles in aqueous solution (samples GS1 and GS3). All remaining formulations were made by directly mixing powders in aqueous medium (samples GS2, GS4, GS5, and GS6). For all samples, the aqueous mixture was vortexed and left on the shaker for 5 h. The fully suspended components were left in the refrigerator for another 3 h. The samples were then placed at −40 °C until they were fully frozen. The frozen samples were placed in a freeze-dryer to obtain a fully dry powder. For each sample, the dry powder was then suspended in an appropriate amount of 0.1 M PBS. This solution was thereafter properly mixed with an aqueous vehicle containing hypromellose and Pluronic L-61, reaching a final concentration of 0.05% (w/v) quercetin and 0.01% (w/v) hypromellose and Pluronic L-61 in the finished product, thus obtaining a viscous spray solution ready to be used.

Four Si-based formulations were prepared and referred to as GS1−GS4. GS5 refers to quercetin (Q) alone; GS6 refers to the Si-NPs devoid of quercetin (P), whereas GS7 indicates the aqueous vehicle (B). Table 1 resumes all of the samples analyzed.

Quercetin Quantification in the Si-Based Phyto-Courier Samples. Standard stock solutions of quercetin were dissolved in 1:1 MeOH/H_2O at the concentration of 0.75−100 μg/mL. All standard solutions were filtered through a 0.22 μm polytetrafluoroethylene (PTFE) syringe filter.

The HPLC system used was a Shimadzu Nexera-i (Kyoto, Japan) chromatograph equipped with a solvent delivery unit (LC-30AD), an autosampler (SIL-30AC), a column oven (CTO-20A), a degasser (DGU-20A5R), and a photodiode array detector (SPD-M20A). Separation was conducted on a Kinetex (4.6 × 250 mm column, 5 μm; Phenomenex, UK). The column temperature was set at 40 °C.

https://dx.doi.org/10.1021/acsnano.0c09488
ACS Nano 2021, 15, 3061−3069

Table 2. List of Primer Pairs Used in This Study and Specific for Two Glutathione Reductase Isoforms (*GR1*-XM_030652414.1 and *GR2*-XM_030624243.1), with Details of the Amplicon Sizes and the Efficiency of Amplification

primer name	sequence (5′→3′)	amplicon size (bp)	amplification efficiency (%)
CsGR1 Fwd	TGCTGTGTTTTCGCAACCAC	80	94.7
CsGR1 Rev	TGTCAACATCGCCATACTGC		
CsGR2 Fwd	TTCCGTTGGCGTCGAAATTG	125	96.9
CsGR2 Rev	AGGCGACAGGGGTAAGATTTAC		

The mobile phase consisted of H_2O containing 0.1% (v/v) trifluoroacetic acid (A) and MeOH (B), at the ratio of 50:50. Elution was performed in isocratic mode; the flow rate was 1.00 mL/min, and the injection volume was 10 μL. The detection wavelength of all standards and samples was in the UV range at λ_{max_1} = 254 nm and at λ_{max_2} = 370 nm. The average retention time was 4.5 min and the total elution time set at 10 min.

Fractions of prepared samples were digested by mixing withdrawn aliquots (0.3 mL) with MeOH at a 1:1 ratio. Samples were vortexed and then filtered through a 0.22 μm (PTFE) syringe filter and moved to amber glass vials prior to injection. Analyses were performed in triplicate per sample.

Plant Growth and Treatments. Plants were grown for 31 days in pots with 1/3 sand and 2/3 potting soil in controlled chambers (60% humidity) with a 16 h light 25 °C/8 h dark 20 °C cycle. The formulations were sprayed for a total of six times on the leaves (the first time when the plants were 10 days old, the second time when they were 17 days old, and then the applications were repeated with an interval of 3−4 days). For young plants with only the first pair of true leaves, the spraying covered the whole leaf area; for adult plants, spraying was performed in the middle of the new leaf clusters and, for older leaves, at the base (to favor absorption via the leaf veins), where the lobes are connected. The soil was covered during spraying to avoid runoff. Three weeks passed from the first application of the formulations to the sampling.

Salt (60 mL of NaCl 250 mM) was applied for the first time when the plants were 17 days old, and then it was supplied to the soil three more times (when the plants were 17, 24, and 27 days old). Control plants received 60 mL of water. The conditions are abbreviated as follows: control (C), buffer alone (B) (*i.e.*, the real control of the formulations since it is composed of the medium in which the Si-NPs are dissolved), phyto-courier alone without quercetin (P), quercetin alone (Q), the four phyto-courier formulations with quercetin (GS1−GS4). Salt stress treatments are indicated with the same abbreviations followed by NaCl.

Hemp leaves were harvested and immediately weighed to determine the fresh weight (FW); the tissues were subsequently put in an oven at 37 °C until constant weight (approximately after 72h) and weighed again to determine the dry weight (DW). From the FW and DW values, the leaf moisture percentage [$M(\%)$] could be calculated as follows:

$$M(\%) = [(\mathrm{FW} - \mathrm{DW})/\mathrm{FW}] \times 100$$

Si Quantification in Hemp Leaves. The dried leaves were milled to a fine powder and mineralized in a microwave oven Multiwave Pro (Anton Paar) by adding 4.5 mL of HCl and 1.5 mL of HNO_3 to 250 mg of dried sample. The mineralization was done at a maximal pressure of 40 bar and at a maximal temperature of 210 °C. For each digestion cycle, a blank and a certified reference material (*Citrus* leaves, NCS ZC 73018, LGC Standards) were added to, respectively, control the cleanliness of the tubes and determine the Si extraction recovery. After the mineralization process, the final volume was adjusted to 25 mL by adding ultrapure water, and then the samples were centrifuged at 4700 rpm for 10 min, filtered through 0.2 μm PTFE filters, and stored at 4 °C until the analysis.

After being diluted, the samples were analyzed by ICP-MS (7900 ICP-MS, Agilent). The quantification of ^{28}Si was performed with a calibration curve between 100 and 2500 μg/L. Blanks and quality control standards were analyzed every 10 samples to ensure the validity of the analytical method. ^{103}Rh was used as internal standard to correct any factor affecting the analyte signal. After measurement, the dilution factor and the recovery factor obtained from the certified reference material were applied. The concentrations were then expressed in micrograms of Si per gram of dried sample.

Extraction of Soluble Sugars and Quantification. Carbohydrates were extracted and quantified as previously reported.[41,42] Briefly, hemp leaves were ground to a fine powder in liquid nitrogen, and 100 mg of material was added to 1 mL of an EtOH/H_2O (80:20, v/v) mixture. Four technical replicates were performed per biological replicate. Four independent biological replicates, each consisting of a pool of mature leaves (sampled at the middle of the stem) from two plants, were performed in the experimental setup. After vortexing and shaking for 30 min at 1400 rpm and at a temperature of 4 °C, the tubes were centrifuged at 17000*g* for 10 min at 4 °C. The supernatant was removed, and the residue was re-extracted with 0.5 mL of the same EtOH/H_2O mixture (80:20, v/v). The supernatant thus obtained was pooled to the first one and evaporated at reduced pressure (Speedvac). The final dried extract was resuspended in 1 mL of ultrapure water and filtered through 0.45 μm PVDF filters before analysis using high-performance anion exchange chromatography coupled with pulsed amperometric detection HPAEC-PAD (Dionex ED 40, Dionex Corp.). The analytical column was a Dionex CarboPac PA-20 (3 × 150 mm) maintained at 35 °C. The mobile phase was online generated with KOH at 0.5 mL min^{-1}. The PAD detection was performed with a gold working electrode and a Ag/AgCl reference electrode, with a data collection rate of 2 Hz. Soluble sugars were quantified using a seven-point calibration curve with standard solutions of galactose, glucose, sucrose, fructose, and raffinose ranging from 1 to 100 μM. The concentrations were expressed in micromole per gram of fresh weight (FW).

RNA Extraction and Gene Expression Analysis. Total RNA was extracted from the youngest pair of fully expanded leaves (right below the stem apex) with the Qiagen RNeasy plant mini kit with the on-column DNase treatment. Extracted RNAs were quantified at the Nanodrop and their integrities checked at the bioanalyzer (all RINs > 7.5). One microgram of RNA was retrotranscribed into cDNA using the ProtoScript II RTase (NEB) and random hexamers. RT-qPCR was carried out in 384-well microplates which were prepared using a liquid handling robot (epMotion, Eppendorf) and run using the Takyon Rox SYBR MasterMix dTTP blueMix in a ViiA7 thermal cycler.[43] The expression was calculated using 2 reference genes (*eTIF4E* and *GAPDH* which geNORM, implemented in qBASE+,[44] identified as sufficient for data normalization). Primers were designed using Primer3Plus (http://www.bioinformatics.nl/cgi-bin/primer3plus/primer3plus.cgi/) and verified with the OligoAnalyzer 3.1 tool from Integrated DNA technologies (http://eu.idtdna.com/calc/analyzer). Primer efficiencies were calculated *via* RT-qPCR using a serial 5-fold dilution of cDNA (25, 5, 1, 0.2, 0.04, 0.008 ng/μL). The primer sequences, amplification efficiencies, and R^2 are shown in Table 2 or have been previously published.[10,43]

Statistics. Data were $\log_{10}$-transformed prior to statistical analysis. Normal distribution of the data was checked using a Shapiro−Wilk test in IBM SPSS statistics v19. Homogeneity of the data was checked with the Levene's test. For data following normal distribution, a one-way ANOVA with Tukey's posthoc text was performed. For data not following normal distribution and not homogeneous, a Kruskal−Wallis test was performed with Dunn's posthoc test.

https://dx.doi.org/10.1021/acsnano.0c09488
ACS Nano 2021, 15, 3061−3069

ASSOCIATED CONTENT

Supporting Information

The Supporting Information is available free of charge at https://pubs.acs.org/doi/10.1021/acsnano.0c09488.

Figures showing the macroscopic phenotypes of hemp plants aged 31 days, the discoloration on the dorsal leaves of hemp aged 20 days and treated with GS3 and GS4, the FW/DW/moisture content of hemp leaves treated or not with the hybrid formulations under control or stress conditions and the Si content in the leaves of plants treated or not with the formulations under control or salt stress conditions (PDF)

AUTHOR INFORMATION

Corresponding Author

Suzanne Saffie-Siebert − *SiSaf Ltd., Guildford GU2 7RE, United Kingdom*; Email: saffie@sisaf.com

Authors

Gea Guerriero − *Environmental Research and Innovation Department, Luxembourg Institute of Science and Technology, L-4940 Hautcharage, Luxembourg*; orcid.org/0000-0001-6586-6997

Flavia Maria Sutera − *SiSaf Ltd., Guildford GU2 7RE, United Kingdom*

Nissim Torabi-Pour − *SiSaf Ltd., Guildford GU2 7RE, United Kingdom*

Jenny Renaut − *Environmental Research and Innovation Department, Luxembourg Institute of Science and Technology, L-4422 Belvaux, Luxembourg*

Jean-Francois Hausman − *Environmental Research and Innovation Department, Luxembourg Institute of Science and Technology, L-4940 Hautcharage, Luxembourg*

Roberto Berni − *TERRA Teaching and Research Center, Gembloux Agro-Bio Tech, University of Liège, 5030 Gembloux, Belgium*

Holly Cherise Pennington − *SiSaf Ltd., Guildford GU2 7RE, United Kingdom*

Michael Welsh − *SiSaf Ltd., Guildford GU2 7RE, United Kingdom*

Ashkan Dehsorkhi − *SiSaf Ltd., Guildford GU2 7RE, United Kingdom*

Lali Ronsoni Zancan − *SiSaf Ltd., Guildford GU2 7RE, United Kingdom*

Complete contact information is available at: https://pubs.acs.org/10.1021/acsnano.0c09488

Author Contributions

G.G. and F.M.S. contributed equally to this work. G.G., F.M.S., and S.S.-S. conceived the idea and designed the experiment. G.G., F.M.S., N.T.-P., H.C.P., M.W., A.D., and L.R.Z. performed the experiments. G.G., F.M.S., N.T.-P., R.B., H.C.P., M.W., A.D., L.R.Z., and S.S.-S. analyzed and interpreted the data. G.G., F.M.S., and S.S.-S. wrote the manuscript. All the authors reviewed the text and agreed with the final manuscript.

Notes

The authors declare the following competing financial interest(s): F.M.S., N.T.-P., H.C.P., M.W., A.D., L.R.Z. are scientists working for SiSaf Ltd, a commercial stage biopharmaceutical Company. S.S.-S. is founder and CEO of SiSaf Ltd.

ACKNOWLEDGMENTS

This work was supported by the Luxembourg National Research Fund (BRIDGES2020/BM/14608886).

REFERENCES

(1) Roy, S. J.; Tucker, E. J.; Tester, M. Genetic Analysis of Abiotic Stress Tolerance in Crops. *Curr. Opin. Plant Biol.* **2011**, *14* (3), 232−239.

(2) Sea Level Rise, Facts and Information. https://www.nationalgeographic.com/environment/global-warming/sea-level-rise/ (accessed 2020-11-10).

(3) Arora, N. K. Impact of Climate Change on Agriculture Production and Its Sustainable Solutions. *Environmental Sustainability* **2019**, *2* (2), 95−96.

(4) Parvin, K.; Hasanuzzaman, M.; Bhuyan, M. H. M. B.; Mohsin, S. M.; Fujita, M. Quercetin Mediated Salt Tolerance in Tomato through the Enhancement of Plant Antioxidant Defense and Glyoxalase Systems. *Plants* **2019**, *8* (8), 247.

(5) Berni, R.; Luyckx, M.; Xu, X.; Legay, S.; Sergeant, K.; Hausman, J.-F.; Lutts, S.; Cai, G.; Guerriero, G. Reactive Oxygen Species and Heavy Metal Stress in Plants: Impact on the Cell Wall and Secondary Metabolism. *Environ. Exp. Bot.* **2019**, *161*, 98−106.

(6) Andre, C. M.; Hausman, J.-F.; Guerriero, G. *Cannabis sativa*: The Plant of the Thousand and One Molecules. *Front. Plant Sci.* **2016**, *7*, 19.

(7) Rea, K. A.; Casaretto, J. A.; Al-Abdul-Wahid, M. S.; Sukumaran, A.; Geddes-McAlister, J.; Rothstein, S. J.; Akhtar, T. A. Biosynthesis of Cannflavins A and B from *Cannabis sativa* L. *Phytochemistry* **2019**, *164*, 162−171.

(8) Flores-Sanchez, I. J.; Verpoorte, R. Secondary Metabolism in *Cannabis*. *Phytochem. Rev.* **2008**, *7* (3), 615−639.

(9) Landi, S.; Berni, R.; Capasso, G.; Hausman, J.-F.; Guerriero, G.; Esposito, S. Impact of Nitrogen Nutrition on *Cannabis sativa*: An Update on the Current Knowledge and Future Prospects. *Int. J. Mol. Sci.* **2019**, *20* (22), 5803.

(10) Guerriero, G.; Behr, M.; Hausman, J.-F.; Legay, S. Textile Hemp *vs.* Salinity: Insights from a Targeted Gene Expression Analysis. *Genes (Basel)* 2017, *8* (10). DOI: 10.3390/genes8100242.

(11) Berni, R.; Mandlik, R.; Hausman, J.-F.; Guerriero, G. Silicon-Induced Mitigatory Effects in Salt-Stressed Hemp Leaves. *Physiologia Plantarum in press*. DOI: 10.1111/ppl.13097.

(12) Guerriero, G.; Hausman, J.-F.; Legay, S. Silicon and the Plant Extracellular Matrix. *Front. Plant Sci.* **2016**, *7*, 463.

(13) Luyckx, M.; Hausman, J.-F.; Lutts, S.; Guerriero, G. Silicon and Plants: Current Knowledge and Technological Perspectives. *Front. Plant Sci.* **2017**, *8*, 411.

(14) Guerriero, G.; Deshmukh, R.; Sonah, H.; Sergeant, K.; Hausman, J.-F.; Lentzen, E.; Valle, N.; Siddiqui, K. S.; Exley, C. Identification of the Aquaporin Gene Family in *Cannabis sativa* and Evidence for the Accumulation of Silicon in Its Tissues. *Plant Sci.* **2019**, *287*, 110167.

(15) Ma, J. F.; Tamai, K.; Yamaji, N.; Mitani, N.; Konishi, S.; Katsuhara, M.; Ishiguro, M.; Murata, Y.; Yano, M. A Silicon Transporter in Rice. *Nature* **2006**, *440* (7084), 688−691.

(16) Luyckx, M.; Hausman, J.-F.; Lutts, S.; Guerriero, G. Impact of Silicon in Plant Biomass Production: Focus on Bast Fibres, Hypotheses, and Perspectives. *Plants* **2017**, *6* (4), 37.

(17) Pulizzi, F. Nano in the Future of Crops. *Nat. Nanotechnol.* **2019**, *14* (6), 507−507.

(18) Fischer, J.; Beckers, S. J.; Yiamsawas, D.; Thines, E.; Landfester, K.; Wurm, F. R. Targeted Drug Delivery in Plants: Enzyme-Responsive Lignin Nanocarriers for the Curative Treatment of the Worldwide Grapevine Trunk Disease Esca. *Advanced Science* **2019**, *6* (15), 1802315.

(19) Rastogi, A.; Tripathi, D. K.; Yadav, S.; Chauhan, D. K.; Živčák, M.; Ghorbanpour, M.; El-Sheery, N. I.; Brestic, M. Application of Silicon Nanoparticles in Agriculture. *3 Biotech* **2019**, *9* (3), 90.

(20) Laane, H.-M. The Effects of Foliar Sprays with Different Silicon Compounds. *Plants* **2018**, *7* (2), 45.
(21) Savvas, D.; Ntatsi, G. Biostimulant Activity of Silicon in Horticulture. *Sci. Hortic.* **2015**, *196*, 66−81.
(22) Bae, H.; Herman, E.; Bailey, B.; Bae, H.-J.; Sicher, R. Exogenous Trehalose Alters *Arabidopsis* Transcripts Involved in Cell Wall Modification, Abiotic Stress, Nitrogen Metabolism, and Plant Defense. *Physiol. Plant.* **2005**, *125* (1), 114−126.
(23) Duman, F.; Aksoy, A.; Aydin, Z.; Temizgul, R. Effects of Exogenous Glycinebetaine and Trehalose on Cadmium Accumulation and Biological Responses of an Aquatic Plant (*Lemna gibba* L.). *Water, Air, Soil Pollut.* **2011**, *217* (1), 545−556.
(24) Luo, Y.; Li, F.; Wang, G. P.; Yang, X. H.; Wang, W. Exogenously-Supplied Trehalose Protects Thylakoid Membranes of Winter Wheat from Heat-Induced Damage. *Biol. Plant.* **2010**, *54* (3), 495−501.
(25) Ma, C.; Wang, Z.; Kong, B.; Lin, T. Exogenous Trehalose Differentially Modulate Antioxidant Defense System in Wheat Callus during Water Deficit and Subsequent Recovery. *Plant Growth Regul.* **2013**, *70* (3), 275−285.
(26) Sadak, M. S. Physiological Role of Trehalose on Enhancing Salinity Tolerance of Wheat Plant. *Bulletin of the National Research Centre* **2019**, *43* (1), 53.
(27) Mostofa, M. G.; Hossain, M. A.; Fujita, M. Trehalose Pretreatment Induces Salt Tolerance in Rice (*Oryza sativa* L.) Seedlings: Oxidative Damage and Co-Induction of Antioxidant Defense and Glyoxalase Systems. *Protoplasma* **2015**, *252* (2), 461−475.
(28) Nuruzzaman, M.; Rahman, M. M.; Liu, Y.; Naidu, R. Nanoencapsulation, Nano-Guard for Pesticides: A New Window for Safe Application. *J. Agric. Food Chem.* **2016**, *64* (7), 1447−1483.
(29) Kurepa, J.; Shull, T. E.; Smalle, J. A. Quercetin Feeding Protects Plants against Oxidative Stress. *F1000Research* **2016**, *5*, 2430.
(30) Pilon, C.; Soratto, R. P.; Broetto, F.; Fernandes, A. M. Foliar or Soil Applications of Silicon Alleviate Water-Deficit Stress of Potato Plants. *Agronomy Journal* **2014**, *106* (6), 2325−2334.
(31) Ma, J. F.; Yamaji, N. Silicon Uptake and Accumulation in Higher Plants. *Trends Plant Sci.* **2006**, *11* (8), 392−397.
(32) Liang, W.; Ma, X.; Wan, P.; Liu, L. Plant Salt-Tolerance Mechanism: A Review. *Biochem. Biophys. Res. Commun.* **2018**, *495* (1), 286−291.
(33) Verelst, W.; Skirycz, A.; Inzé, D. Abscisic Acid, Ethylene and Gibberellic Acid Act at Different Developmental Stages to Instruct the Adaptation of Young Leaves to Stress. *Plant Signaling Behav.* **2010**, *5* (4), 473−475.
(34) Baran-Rachwalska, P.; Torabi-Pour, N.; Sutera, F. M.; Ahmed, M.; Thomas, K.; Nesbit, M. A.; Welsh, M.; Moore, C. B. T.; Saffie-Siebert, S. R. Topical SiRNA Delivery to Anterior Eye Using Novel Hybrid Silicon-Lipid Nanoparticle Delivery System. *J. Controlled Release* 2020. DOI: 10.1016/j.jconrel.2020.07.004.
(35) Pellegrini, V.; Fuso, F.; Lorenzi, G.; Allegrini, M.; Diligenti, A.; Nannini, A.; Pennelli, G. Improved Optical Emission of Porous Silicon with Different Postanodization Processes. *Appl. Phys. Lett.* **1995**, *67* (8), 1084−1086.
(36) Bellet, D.; Canham, L. Controlled Drying: The Key to Better Quality Porous Semiconductors. *Adv. Mater.* **1998**, *10* (6), 487−490.
(37) Canham, L. T.; Cullis, A. G.; Pickering, C.; Dosser, O. D.; Cox, T. I.; Lynch, T. P. Luminescent Anodized Silicon Aerocrystal Networks Prepared by Supercritical Drying. *Nature* **1994**, *368* (6467), 133−135.
(38) Saffie-Siebert, R.; Ogden, J.; Parry-Billings, M. Nanotechnology Approaches to Solving the Problems of Poorly Water-Soluble Drugs. *Drug Discovery World* **2005**, *6*, 71−76.
(39) Aston, R.; Saffie-Siebert, R.; Canham, L.; Ogden, J. Nanotechnology Applications for Drug Delivery. *Pharmaceutical Technology Europe* **2005**, *17* (4), 21−28.
(40) Bossert, D.; Urban, D. A.; Maceroni, M.; Ackermann-Hirschi, L.; Haeni, L.; Yajan, P.; Spuch-Calvar, M.; Rothen-Rutishauser, B.; Rodriguez-Lorenzo, L.; Petri-Fink, A.; Schwab, F. A Hydrofluoric Acid-Free Method to Dissolve and Quantify Silica Nanoparticles in Aqueous and Solid Matrices. *Sci. Rep.* **2019**, *9* (1), 7938.
(41) Guignard, C.; Jouve, L.; Bogéat-Triboulot, M. B.; Dreyer, E.; Hausman, J.-F.; Hoffmann, L. Analysis of Carbohydrates in Plants by High-Performance Anion-Exchange Chromatography Coupled with Electrospray Mass Spectrometry. *J. Chromatogr A* **2005**, *1085* (1), 137−142.
(42) Guerriero, G.; Giorno, F.; Folgado, R.; Printz, B.; Baric, S.; Hausman, J.-F. Callose and Cellulose Synthase Gene Expression Analysis from the Tight Cluster to the Full Bloom Stage and during Early Fruit Development in *Malus* × *domestica*. *J. Plant Res.* **2014**, *127* (1), 173−183.
(43) Mangeot-Peter, L.; Legay, S.; Hausman, J.-F.; Esposito, S.; Guerriero, G. Identification of Reference Genes for RT-QPCR Data Normalization in *Cannabis sativa* Stem Tissues. *Int. J. Mol. Sci.* **2016**, *17* (9), 1556.
(44) Hellemans, J.; Mortier, G.; De Paepe, A.; Speleman, F.; Vandesompele, J. QBase Relative Quantification Framework and Software for Management and Automated Analysis of Real-Time Quantitative PCR Data. *Genome Biology* **2007**, *8* (2), R19.

https://dx.doi.org/10.1021/acsnano.0c09488
ACS Nano 2021, 15, 3061−3069